



Flight Performance Analysis for an RV-8 Experimental Aircraft

Brian D. Wendt

Mechanical Engineering

The University of Iowa

Iowa City, Iowa

ME:5149 Propulsion Engineering

Professor Albert Ratner

2401 Seamans Center

Iowa City, Iowa 52242

December 2016

Acknowledgments

Thanks to my parents, for always indulging my flights of fancy.

This report is available in electronic form at:
briandwendt.github.io

Abstract

A flight performance analysis was carried out on a Van's RV-8 kit aircraft as a means of reducing data uncertainty by identifying data acquisition errors during its mandatory flight test phase. Standard plots were produced for the aircraft's drag polar, thrust required, power required, and power available. Maximum velocity was estimated at several cruising altitudes. Reasonable estimations were used in lieu of concrete data for Oswald efficiency factor and zero-lift parasite drag, and a numerical method was employed to estimate propeller efficiency. The results compared favorably to the manufacturer's published performance data, validating this approach for aircraft homebuilders and preliminary design studies.

1 Introduction

The reduction of data uncertainty during the flight testing of an experimental aircraft is a constant concern for both pilots and engineers [1]. This applies whether the test article is a high-value commercial prototype or a small homebuilt kit plane. For the homebuilder, a simple performance analysis can be undertaken to provide reasonable targets and expectations for the test data so that gross errors can be more easily identified and eliminated.

The objective of this project was to complete a flight performance analysis for a Van's RV-8 experimental aircraft using software tools, aircraft specifications, and mathematics that are accessible to the average homebuilder. The methods used stem directly from the physical laws governing aircraft flight, and produce characteristic plots familiar to industry or academia. The results are easily interpreted and immediately useful for predicting aircraft performance on the first flight.

2 Test Aircraft

The aircraft used for this analysis was a Van's RV-8 experimental kit plane, modified slightly from the original design with the addition of a "fastback" aft turtledeck and bubble canopy (Fig. 1).

2.1 Van's RV-8

An RV-8 is a two-place tandem-seat sport airplane, sold as a kit by Vans Aircraft, Inc. in Aurora, Oregon. It is one of nearly a dozen aircraft designs offered by Vans, and one of hundreds of kit aircraft models available worldwide. The "R" and "V" in the model name stand for Richard VanGrunsven, or "Van," the company's founder and chief designer.

RVs are built primarily from aluminum alloys, using industry-standard techniques and processes that have been proven in over 70 years of aircraft construction.

The powerplant for the particular RV-8 aircraft analyzed for this project was a Lycoming IO-360, four-cylinder, piston engine rated at 180 horsepower at 2700 rpm. The propeller was a Hartzell two-blade, constant-speed, aluminum propeller with a blade diameter of 74 inches.



Figure 1. RV-8F “Fastback” Experimental Aircraft with Lycoming Engine

2.2 Experimental Category

All US-registered aircraft must be issued an Airworthiness Certificate by the FAA. Most general-aviation airplanes are issued Standard airworthiness certificates, and might be classified as Acrobatic, Utility, Transport, etc. Amateur-built kit aircraft are issued Special airworthiness certificates, and are classified under the Experimental category. All kitplanes must be thoroughly inspected by an FAA Inspector or Designated Airworthiness Representative to ensure that their design, materials and construction comply with industry-standard criteria for safety.

The Experimental Aircraft Association, or EAA, is a large and diverse organization which supports aircraft builders, pilots, manufacturers and enthusiasts, promotes safety, and operates outreach programs to introduce the young and old to the wonders of flight.

EAA's annual "Airventure" Oshkosh air show is one of the premier aviation gatherings in the world.

3 Analysis Toolset

All calculations were completed and plots were generated using the Python programming language and the web-browser-based Jupyter Notebook (Fig. 2). The Jupyter Notebook allows Python code, L^AT_EX mathematical expressions, data visualizations, and explanatory HTML notes to inhabit the same document, so that methods and results can be easily shared and replicated.

Python's NumPy scientific computing library was used to handle arrays and provide accurate physical constants. The `matplotlib` library was used to generate plots, and the `seaborn` visualization library provided plot aesthetics. All software tools with the exception of `seaborn` are available in the free Anaconda Python distribution provided by Continuum Analytics.

All of the calculations and plots for this analysis can be referenced online at:
<https://github.com/briandwendt/Flight-Performance-Analysis>.

4 The Standard Atmosphere

The physical characteristics of the atmosphere — pressure, temperature, density, humidity, and so on — can change seasonally, daily, even hourly. Since all of the flight performance parameters of an aircraft are derived from the medium in which it operates, a standard is needed for consistency and comparison purposes.

Although several atmospheric standards exist, the flight testing community and the FAA use the 1962 U.S. Standard Atmosphere as the reference for aircraft performance [1]. For this analysis, the `scikit-aero` Python package was used to provide accurate atmospheric data for lift and drag calculations [2]. This package is based on the 1976 U.S. Standard Atmosphere, which differs from its 1962 counterpart only above 32 km — altitudes well above those at which most airbreathing aircraft normally operate.

The 1962 U.S. Standard Atmosphere assumes that the air is a perfect, dry gas, with a temperature at sea level of 15°C, a pressure of 29.92 inches of mercury, and a linear temperature lapse rate with altitude to the top of the tropopause at 36,089 feet [3].

5 Aircraft Equations of Motion

Aircraft performance can be subdivided into two distinct categories, static and dynamic. Static performance, in which the airplane is considered to be in "steady-state" flight,

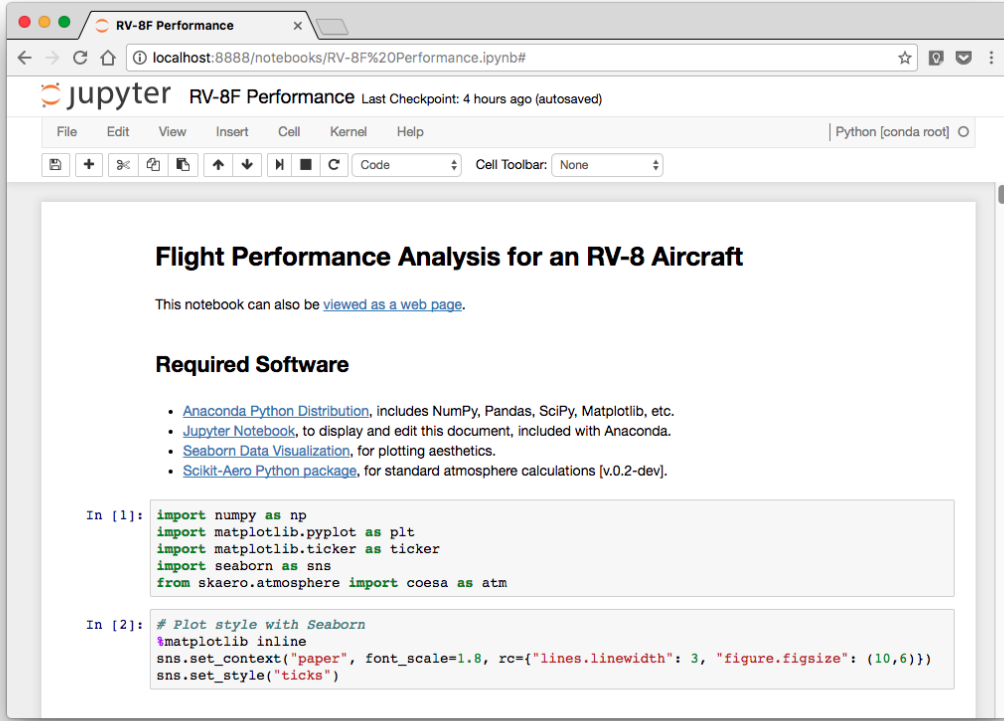


Figure 2. Jupyter Notebook Python environment running in a web browser

occurs when the sum of all the forces acting upon the aircraft results in zero acceleration in any axis. Static performance parameters include such things as maximum velocity, rate of climb, time to climb, maximum altitude, range and endurance. Dynamic performance occurs when the forces acting on the aircraft are not in equilibrium, resulting in a net acceleration. Dynamic parameters include takeoff and landing performance, turning flight, and accelerated or “zoom” climbs [4].

Fig. 3 shows a two-dimensional free-body diagram for an airplane in translational flight. The four force vectors extending from the aircraft center of mass are (1) Lift L , perpendicular to the flight path, (2) Drag D , parallel to the flight path, (3) Weight W , which acts always toward the center of the earth, and (4) Thrust T , which is inclined at some angle α_T relative to the flight path.

The flight path in this case (a shallow climb) is inclined above the horizontal by some angle θ , and the extended chord line of the wing is at an angle of attack α above the flight path (and thus the free stream flow). Summing the forces parallel to the flight path results in

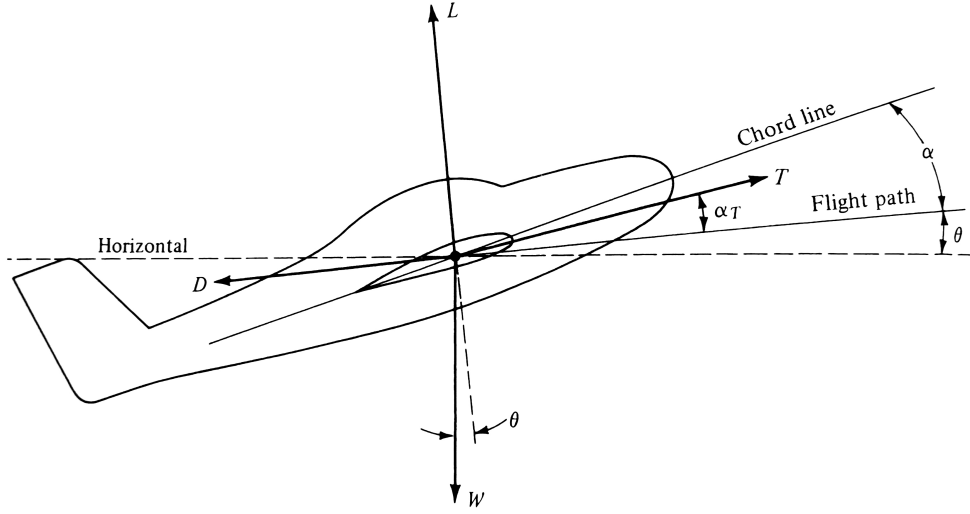


Figure 3. Forces on an aircraft in flight [4]

$$\sum F_{\parallel} = T \cos \alpha_T - D - W \sin \theta \quad (1)$$

and the forces perpendicular to the flight path are

$$\sum F_{\perp} = L + T \sin \alpha_T - W \cos \theta \quad (2)$$

If the aircraft is assumed to be in level, unaccelerated flight, the angle θ between the flight path and the horizontal would go to zero, resulting in the following relations:

$$T \cos \alpha_T = D \quad (3)$$

$$L + T \sin \alpha_T = W \quad (4)$$

The situation can be further simplified for most conventional airplanes (including the RV-8) by assuming that α_T is small enough that $\cos \alpha_T \approx 1$ and $\sin \alpha_T \approx 0$. Thus for unaccelerated level flight, Eqs. (1) and (2) become simply

$$T = D \quad (5)$$

$$L = W \quad (6)$$

In this state, the total drag of the aircraft is exactly balanced by its thrust, and its weight is exactly balanced by the lift force. These relations offer a starting point for the calculation of an airplane's static performance parameters.

6 Drag Polar

Aerodynamic data for a given airplane is packaged in the form of a drag polar, either as a plot or as a set of equations. The drag polar is simply an representation of the relationship between an aircraft's lift versus its drag, and is the basis for all of an airplane's performance calculations [5].

The total drag coefficient of a complete airplane, C_D , can be expressed as the sum of the zero-lift parasite drag coefficient $C_{D,0}$ and the coefficient of drag due to lift $C_{D,i}$, which includes both the induced drag and the increment of parasite drag generated by the wing when operating at angles of attack other than the zero-lift angle, $\alpha_{L=0}$ [4].

$$C_D = C_{D,0} + C_{D,i} \quad (7)$$

The coefficient of drag due to lift is designated by

$$C_{D,i} = \frac{C_L^2}{\pi e AR} \quad (8)$$

where C_L is the coefficient of lift, AR is the aspect ratio of the wing planform, and e is called the *Oswald efficiency factor*, which is a correction for the drag due to lift on a wing with a lift distribution other than an ideal elliptical wing of the same aspect ratio. For unaccelerated, level flight, the coefficient of lift for an airplane is given by

$$C_L = \frac{W}{\frac{1}{2}\rho_\infty V_\infty^2 S} \quad (9)$$

where W is the aircraft weight, ρ_∞ is the static air density, V_∞ is the free-stream velocity, and S is the reference area, taken here to be the total area of the wing planform. Thus, the drag polar equation becomes

$$C_D = C_{D,0} + \frac{C_L^2}{\pi e AR} \quad (10)$$

6.1 Drag Data for the RV-8

Fig. 4 shows the drag polar produced for the RV-8 test aircraft. To create this plot, several of the variables in the lift and drag equations above had to be calculated or assumed. Although Raymer and others [5] [6] provide methods to reasonably estimate the Oswald efficiency factor and zero-lift drag coefficient for conventional airplanes, this analysis relied on data acquired during a 1993 flight test of a similar aircraft, the Van's RV-6A [7].

The RV-6A is a tricycle-gear, two-seat piston airplane, with side-by-side seating rather than the tandem seating of the RV-8. The assumption was made that the zero-

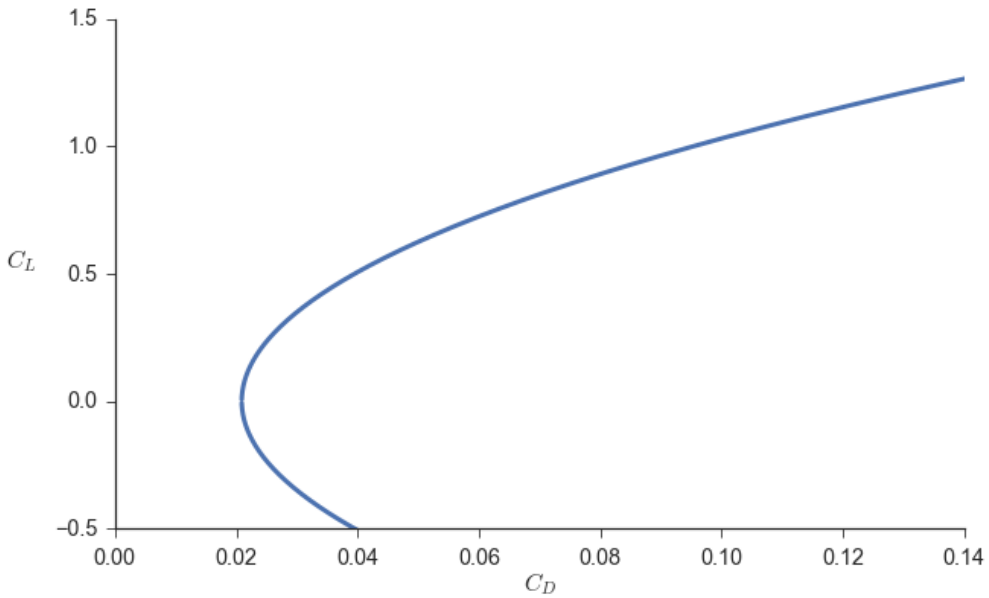


Figure 4. RV-8 Drag Polar, 1800 lbs, Sea Level

lift drag of the RV-8 would be slightly lower than that of the RV-6A, due to the RV-8's smaller frontal area.

Table 6.1 lists the aircraft specifications and assumed aerodynamic values used for the calculation of the RV-8's drag polar. Basic dimensions for the aircraft were obtained from the manufacturer's website, and gross weight was assumed for all plots. The velocity variable was taken to be a range of values between roughly 60 and 220 knots true airspeed, a reasonable assumption for the speed range of a light aircraft.

Table 1. RV-8 Specifications and Aerodynamic Data

| | |
|--|---------------------|
| Wing span, b | 24 ft |
| Wing area, S | 116 ft ² |
| Aspect ratio, AR | b^2/S |
| Gross weight, W | 1800 lbs |
| Free Stream Velocity, V | [100...370] ft/s |
| Oswald efficiency factor, e | 0.86 |
| Zero-lift parasite drag coefficient, $C_{D,0}$ | 0.0209 |

7 Total Drag or Thrust Required

Using the drag polar data obtained above, it is possible to calculate the various performance parameters of the aircraft. The first of these is the thrust required to maintain unaccelerated, level flight at a given altitude. For steady-state flight, thrust must equal drag and lift must balance weight, thus

$$T = D = \frac{1}{2} \rho_{\infty} V_{\infty}^2 S C_D \quad (11)$$

$$L = W = \frac{1}{2} \rho_{\infty} V_{\infty}^2 S C_L \quad (12)$$

Dividing thrust by weight and canceling terms results in

$$\frac{T}{W} = \frac{C_D}{C_L} \quad (13)$$

Multiplying both sides of Eqn. (13) by the weight gives the *thrust required* T_R as

$$T_R = \frac{W}{C_L/C_D} \quad (14)$$

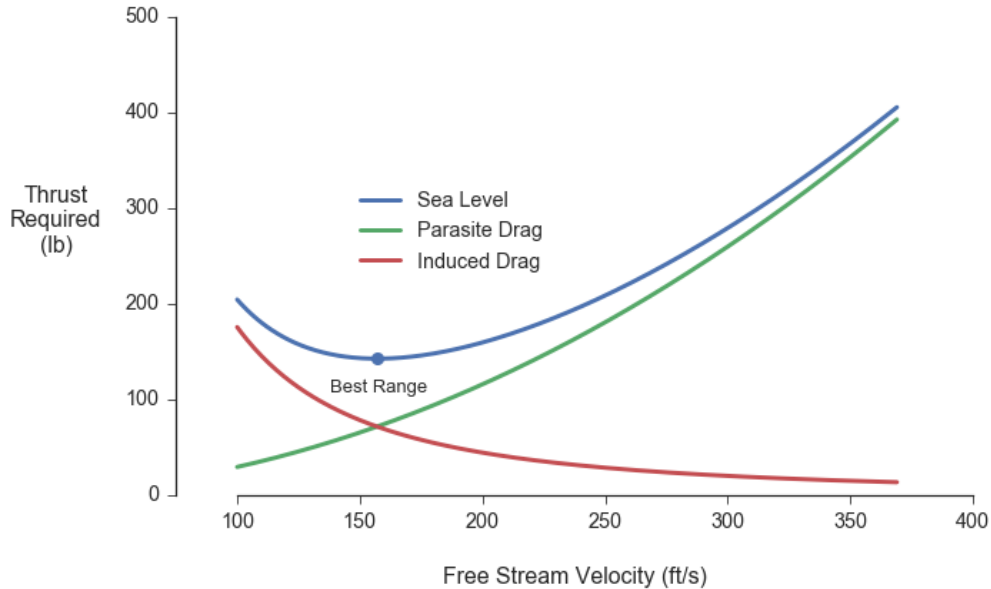


Figure 5. RV-8 Thrust Required (Total Drag) with Parasite and Induced Drag

Fig. 5 shows a plot of the thrust required at sea level for the RV-8. Note that the total drag or thrust required is the sum of the induced drag and the parasite drag, also shown. The minimum value of the thrust required curve, indicated by the blue dot, is the point

of minimum drag and highest aerodynamic efficiency. For a propeller-driven airplane, this point defines the required velocity for achieving *maximum range* at that altitude. Fig. 6 shows the effect of altitude on thrust required.

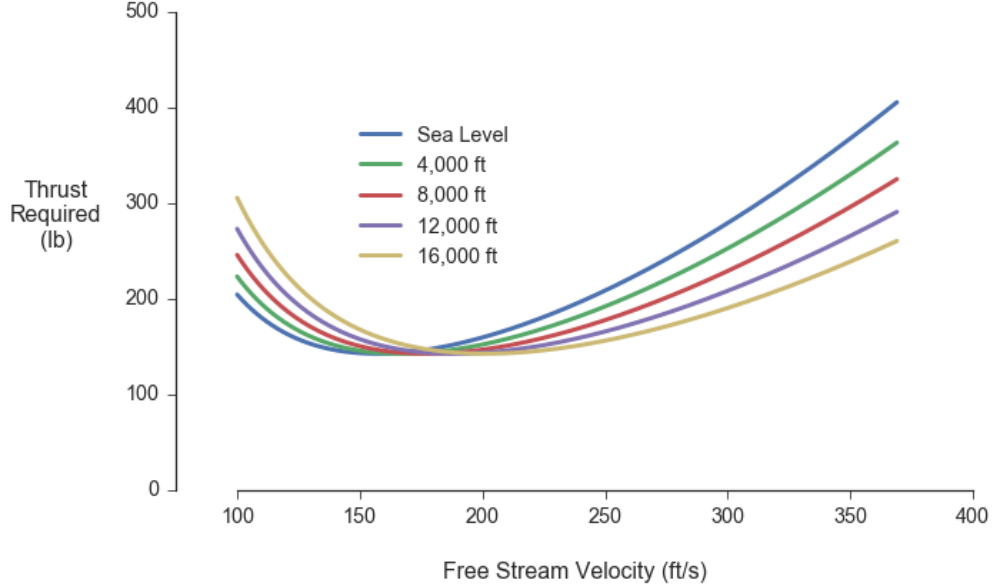


Figure 6. RV-8 Thrust Required, Sea Level to 16,000 feet

8 Power Required

The thrust required curve is immediately useful for jet aircraft, since conventional jet engines are rated in terms of thrust. Piston engines, such as the Lycoming IO-360 in the RV-8, are typically rated in terms of brake horsepower, measured at the output shaft. For piston-driven airplanes, then, the power required and power available curves are more relevant [4]. Power is defined as energy (or work) per unit time, thus

$$\text{Power} = \frac{\text{energy}}{\text{time}} = \frac{\text{force} \times \text{distance}}{\text{time}} = \text{force} \times \frac{\text{distance}}{\text{time}}$$

Since velocity V is distance per unit time, power P can be defined as:

$$P = FV \tag{15}$$

For an airplane in level, unaccelerated flight, at a given altitude, with velocity V_∞ and thrust required T_R , the *power required* is given as

$$P_R = T_R V_\infty \tag{16}$$

Fig. 7 shows a plot of the RV-8's thrust horsepower required versus true airspeed, measured in knots. Note that the minimum point on this curve (the blue dot) represents the airspeed for *maximum endurance* in a propeller-driven airplane. Fig. 8 shows the effect of altitude on the power required curve.

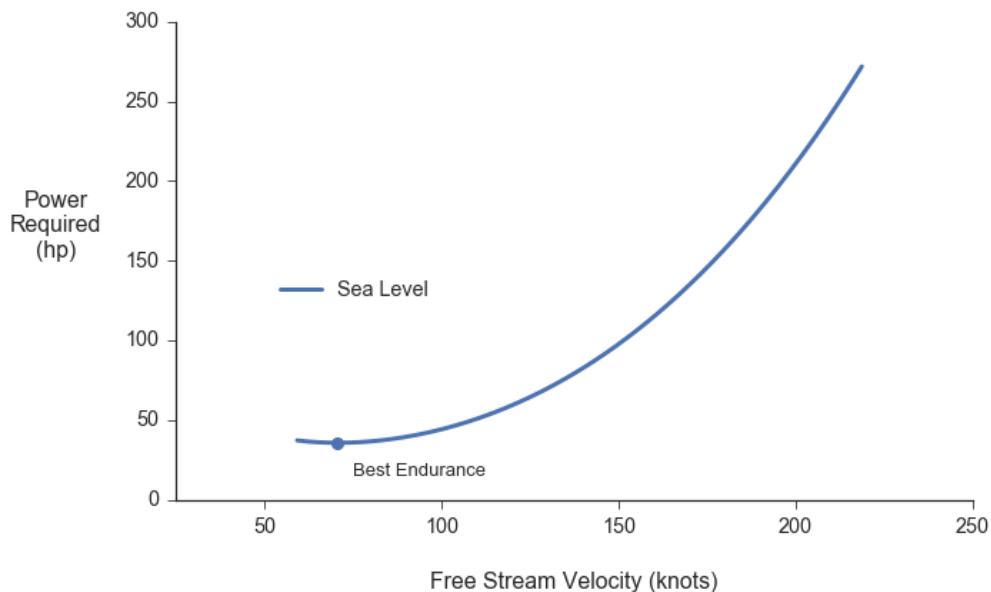


Figure 7. RV-8 Power Required, Sea Level

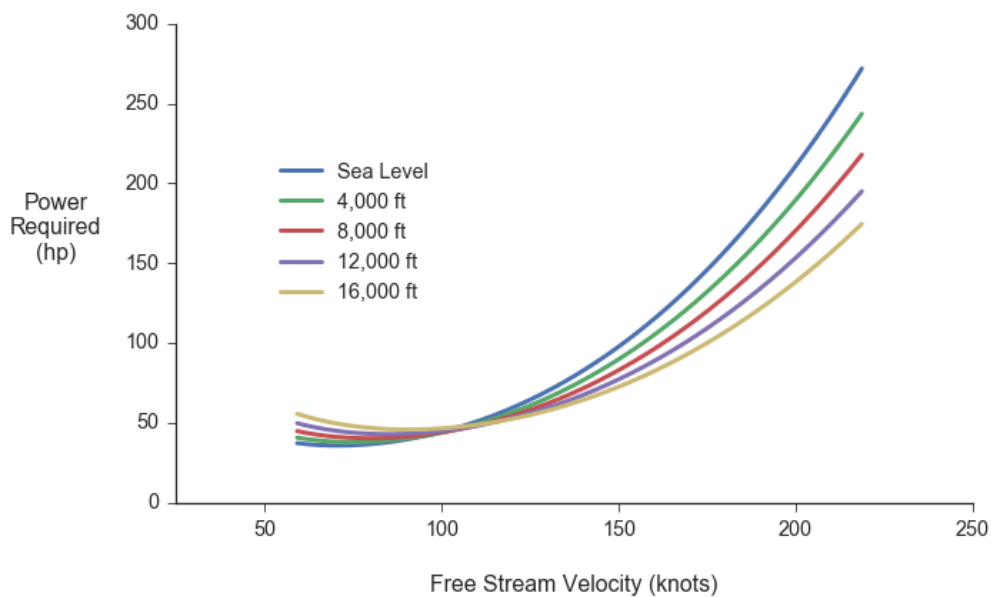


Figure 8. RV-8 Power Required, Sea Level to 16,000 feet

9 Power Available and Maximum Velocity

It is important to note that power required P_R is solely dependent on the aerodynamics of the airplane design — the drag polar. The *power available* P_A , conversely, is a function of the propulsion system. The power output of a piston aircraft engine is typically measured at the crankshaft. This is the brake horsepower available BHP_A from the engine. Converting BHP_A into thrust to propel the airplane, however, must be accomplished by the propeller. The propeller efficiency η , therefore, must be taken into account when calculating the *thrust horsepower available* THP_A , which is given as

$$THP_A = \eta BHP_A \quad (17)$$

9.1 Piston-Engine Altitude Performance

Since mass flow into an engine is dependent on air density, brake horsepower output of a normally-aspirated piston powerplant must therefore decrease with altitude. Fig. 10 (see Appendix) shows the Lycoming IO-360-M1B altitude performance chart, which indicates roughly a 10-hp reduction in BHP_A at full throttle for every 2,000 feet of altitude. Engine altitude performance can also be estimated from Eqn. (18), attributed to the Wright Aeronautical company (circa 1934), which indicates that at 20,000 feet, a normally-aspirated engine outputs less than half of its sea-level-rated brake horsepower [5].

$$P_A = P_{SL} \left(\frac{\rho}{\rho_0} - \frac{1 - \rho/\rho_0}{7.55} \right) \quad (18)$$

Piston engine performance can, of course, be improved by installing a supercharger or turbocharger, both of which increase the intake manifold pressure, however this modification is not installed on the test RV-8, nor does the airframe manufacturer recommend doing so.

9.2 Propeller Efficiency

A propeller is simply a rotating wing, with an airfoil selected to generate thrust, and as such it is designed to be most efficient at some specific flight condition (e.g. climb, cruise, etc.). Propeller performance is a function of the blade airfoil chord, blade diameter, blade pitch, rpm and free-stream velocity [5]. Thus, the propeller efficiency is reduced when not operated at its design conditions.

Computing propeller performance from the raw inputs listed above is beyond the scope of this analysis, and indeed could be the subject of its own study. For this preliminary aircraft performance analysis, a simple and reasonably accurate method of estimating propeller efficiency η was all that was required.

Solies [8] has derived a simple, five-step numerical method for estimating η using only the blade diameter, free-stream velocity, air density and engine brake horsepower as inputs. A reasonable guess for η is used for the first iteration (0.9 was used for this analysis), and the algorithm typically converges within ten or twelve iterations, given a 0.0001% convergence criterion. More details on this procedure are available in the Jupyter Notebook mentioned in Section 3.

9.3 Maximum Velocity

Fig. 9 shows the power required curves for sea level and 8,000 feet (in blue and green), along with the thrust horsepower available curves for both altitudes (in red). The intersection of the THP available curve with the power required curve is the point of maximum velocity V_{max} at that altitude. So, at sea level, the maximum speed attainable is roughly 181 knots, and at 8,000 feet, V_{max} is about 177 knots. These numbers compare favorably to the manufacturer's published data of 213 mph (185 knots) at sea level and 203 mph (176 knots) at 8,000 feet [9].

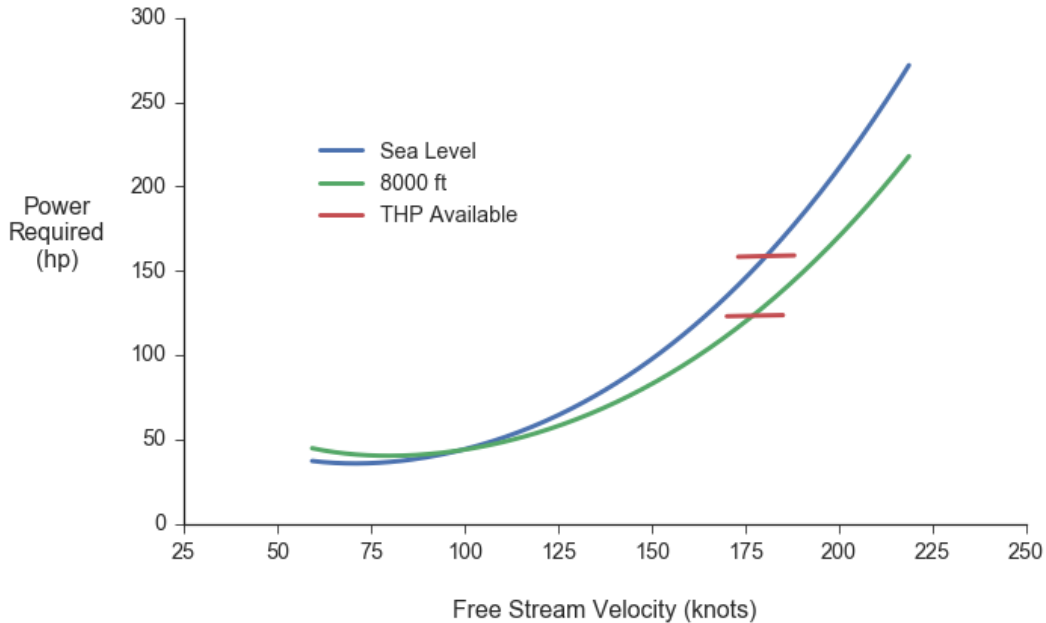


Figure 9. Thrust Horsepower Available, Sea Level and 8,000 ft

10 Conclusions and Further Study

Although this type of analysis relies on several estimated parameters for drag and efficiency, the results are acceptable to predict the performance of a light aircraft such as

the RV-8. Further computations could also be made using the existing drag polar data to estimate the best rate-of-climb airspeed, maximum range and endurance, and takeoff and landing performance.

Future improvements to this method might include the use of computational fluid dynamics (CFD) software to better estimate the zero-lift drag coefficient and Oswald efficiency number. Propeller performance curves could be obtained from the manufacturer to improve the accuracy of the propeller efficiency at various airspeeds and altitudes.

However, it seems clear that this method as presented is sufficiently accurate for giving insight to the average kit plane homebuilder on aircraft performance, and helping to identify gross data collection errors during flight test.

References

- [1] R. D. Kimberlin, *Flight Testing of Fixed-Wing Aircraft*. Reston, Va.: American Institute of Aeronautics and Astronautics, 2003.
- [2] J. L. Cano, “scikit-aero.” <https://github.com/AeroPython/scikit-aero>, 2016.
- [3] COESA, “Standard Atmosphere, 1962,” pp. 1–296, Dec. 1962.
- [4] J. D. Anderson, *Introduction to Flight*. New York: McGraw-Hill, 5th ed., 2005.
- [5] D. P. Raymer, *Aircraft Design: A Conceptual Approach*. Reston, Va: American Institute of Aeronautics and Astronautics, 4th ed., 2006.
- [6] M. Nita and D. Scholz, “Estimating the Oswald Factor from Basic Aircraft Geometrical Parameters,” in *German Aerospace Congress*, pp. 1–19, Dec. 2012.
- [7] R. Scott and C. J. Stevens, “Aircraft Performance Report: RV-6A,” 1993. http://cafe.foundation/v2/pdf_cafe_apr/RV-6A%20Final%20APR.pdf.
- [8] U. P. Solies, “Numerical Method for Estimation of Propeller Efficiencies,” *Journal of Aircraft*, vol. 31, pp. 996–998, July 1994.
- [9] Van’s Aircraft Inc., “RV8/8A Performance.” <http://www.vansaircraft.com/public/rv8perf.htm>. Accessed: 2016-11-27.

Appendix

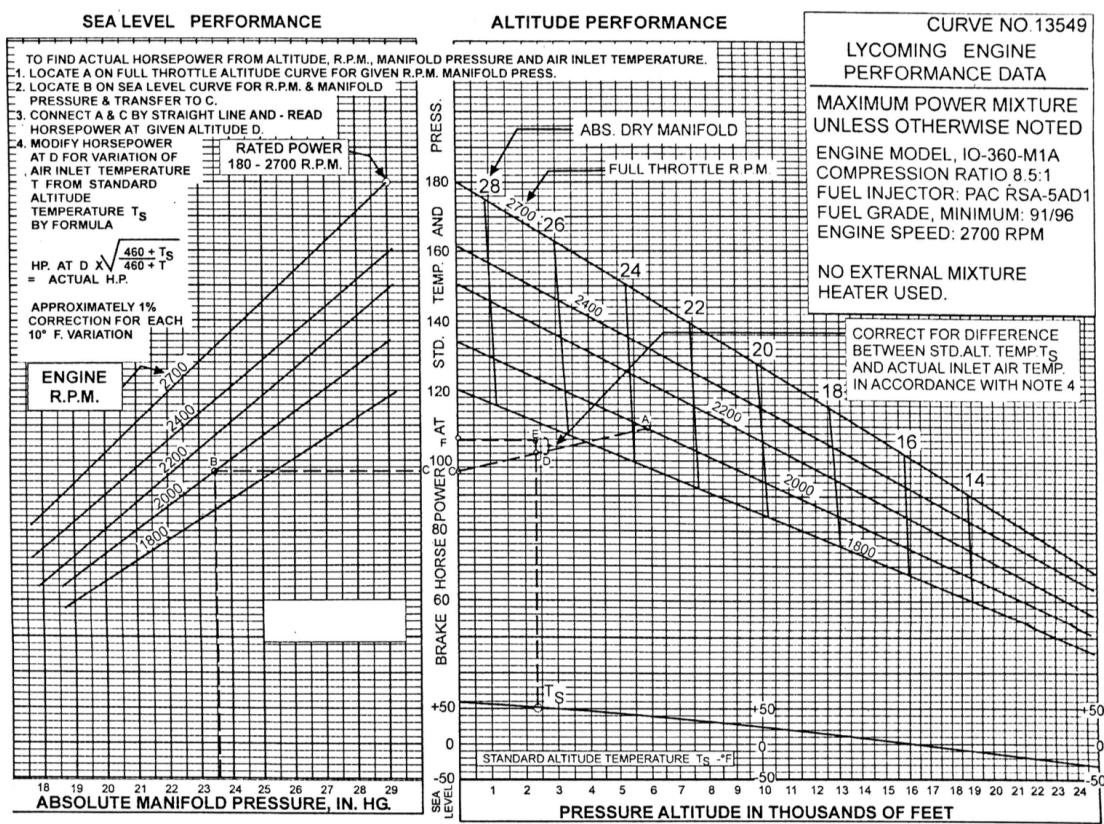


Figure 10. Lycoming IO-360-M1B Performance Chart